Effects of Accretion Column Structure on Beam Shapes

D.A. Leahy
Department of Physics &Astronomy , University of Calgary, Calgary, Alberta T2N 1N4, Canada

A model calculation for the beam pattern from a filled-cone shaped accretion column is generalized to include spatially-dependent emissivities. The emission region is also generalized to include emission from the neutron star surface heated by the emission from the sides of the accretion column. Gravitational light-bending and shadowing effects are included in the calculation. The resulting beaming patterns are calculated and compared to the previous calculations of beaming patterns from simpler geometries and emissivities.

1. INTRODUCTION

An X-ray pulsar is an accreting neutron star in a binary system. It emits X-ray pulsations due to rotation: the beam pattern from the bright emission region rotates past the observer's line-of-sight. The accretion flow from the companion star has sufficient conductivity that inside the magnetosphere, it follows magnetic field lines to the neutron star surface. This results in two X-ray emission regions: one for each magnetic pole. The emission region may be on the neutron star surface (called a polar cap) or form an accretion column extending vertically above the neutron star surface. The pulse shapes produced by polar cap models have been considered by, e.g. [1], and references therein. The pulse shapes produced by accretion column models are considered by [2], [3], [4]. The geometrical model here for the accretion column is a filled cone with both the top and sides emitting and producing pencil and fan beams, respectively beamed along the surface normal and approximately perpendicular to the surface normal. It also includes emission from the neutron star surrounding the base of the column which is due to heating by radiation from the sides of the accretion column.

The filled cone model was applied successfully to explain the pulse shape of Her X-1 by [5], then to constrain the mass-radius relation of the neutron star by [6]. The purpose of this paper is to generalize the filled cone model of [5] to include a height-dependent emissivity in the cone, and emission from the neutron star surface surrounding the base of the accretion column. All of the calculations here were done for neutron stars of 1.4 solar masses. Section 2 below describes the accretion column model, and its generalization from previous models. Section 3 describes resulting beam patterns calculated using this model. Section 4 contains a discussion and summary of the results.

2. THE EMISSIVITY MODEL

Fig. 1 shows the basic geometry used here for the beam pattern calculations. The emission region is a cone-shaped region with emitting top and sides, with the apex of the cone at the center of the neutron star. Only the part of the cone extending above the neutron star surface emits radiation. There is also a surface emission ring surrounding the base of the cone, which should be present due to emission from the part of the surface heated by radiation from the sides of the cone. Since the emitting plasma is constrained by the strong magnetic field, the sides of the cone are not straight but follow dipole magnetic field lines.

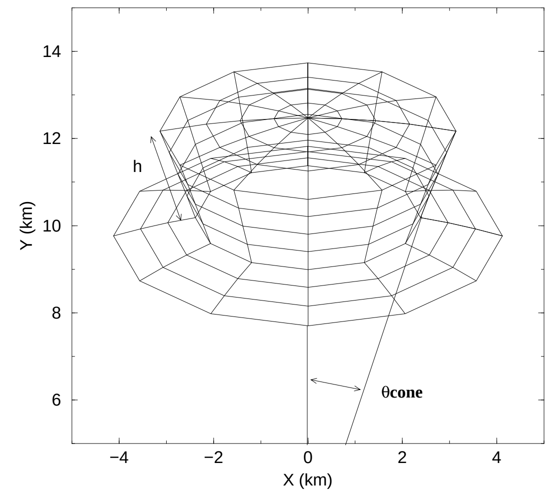

Figure 1: Emission region geometry: the cone is due to matter incoming from the disk along magnetic field lines, with the top due to the standoff shock. The ring is the neutron star surface heated by radiation from the sides of the cone. The cone-top and the ring produce pencil beam patterns: beamed along the radial direction; the cone-side produces a fan beam pattern: beamed tangential to the surface. Here, the neutron star radius is $R = 12$ km; the cone sides follow dipole field lines; the cone height is $H = 0.2R$; the cone half-angle is $\theta_c = 0.2$ rad at base; and the surface ring outer angle is 0.35 rad. The view shown is with the observer at $\theta_1 = 60^\circ$ to the cone axis.

Photons from the surface of the emission region propagate to the observer along geodesics in the Schwarzschild metric (only slowly rotating neutron stars are considered here). Fig. 2 illustrates the magnitude of the resulting bending of light paths for a neutron star of 1.4 solar masses and 3 different radii. The smallest radius shown, 7.28 km, is that for which

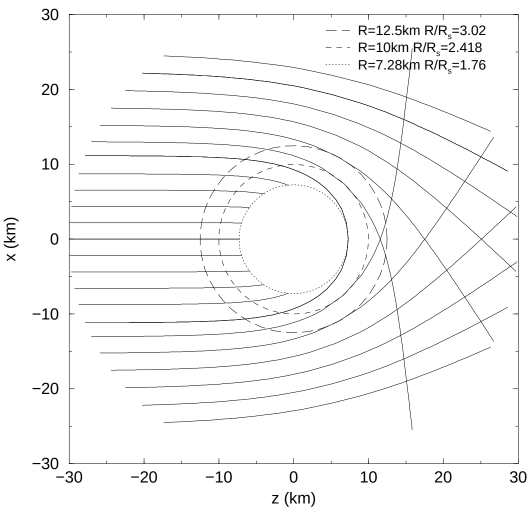

Figure 2: Light rays (solid lines) around a 1.4 $M_\odot$ neutron star. Three different radii of neutron stars are illustrated. Light-bending [2] results in magnification and distortion of the emission regions.

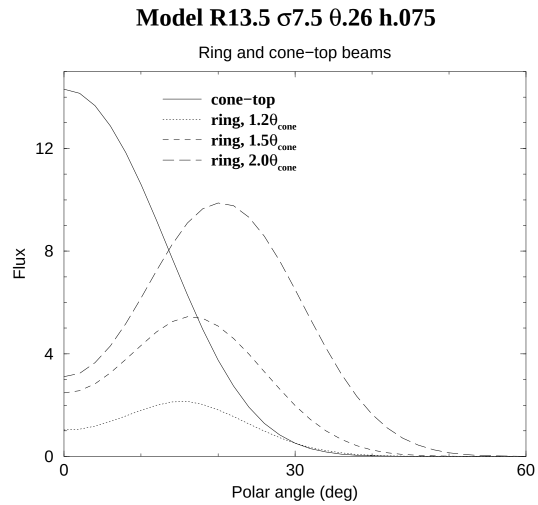

Figure 3: Beam pattern of top and ring regions, R=13.5km: dependence on ring size. The dip in beam pattern from the ring for polar angles less than 20° is due to shadowing of the ring by the cone.

an observer can see just the entire surface of the neutron star. Realistic equations of state for matter at high density predict radii in the range $\sim 9-16$km for a mass of 1.4 solar masses.

In addition to a surface geometry, an emissivity must be specified in order to compute a beam pattern observed at infinity from the emission surface. The anisotropy of the basic emission and absorption properties in the strong magnetic fields ($\sim 10^{12}$ Gauss) found in pulsating neutron stars, results in a dependence of the emissivity on emission angle. The radiation transfer problem in such an environment has not been solved fully yet (e.g. [7], [8]). The approach taken here is to use a phenomenological model for the surface emissivity. A Gaussian function is used for the dependence on the angle to the surface normal, δ.

$$f1(\delta) = exp(-\delta^2/2\sigma^2) \quad (1)$$

The vertical structure of the accretion column is not known either, so another phenomelogical description is used here: the dependence of emissivity on height, h, in the accretion column is specified by:

$$f2(h) = (1 + (H-h)/H)^\alpha \quad (2)$$

with H the height of the top of the column. The emissivity also depends on location of the emitting point on the top of the accretion column or location in the surface emission ring. For an axisymmetric column and ring, position is specified by the angle from the magnetic axis, θ. The emissivity dependence on θ is specified by:

$$f3(\theta) = (1 + (\theta 2 - \theta)/(\theta 2 - \theta 1))^\beta \quad (3)$$

with $\theta 2$ and $\theta 1$, the inner and outer limits of the cone-top or of the surface ring.

A dependence of emissivity on azimuthal angle with respect to the magnetic axis is expected due to the azimuthal dependence of efficiency for matter threading onto magnetic field lines from the inner accretion disk. Here is used a dependence on ϕ of:

$$C(\phi) = (1 + a_c \cos^2((\phi - \phi_2)/2)) \quad (4)$$

3. RESULTS OF BEAM PATTERN CALCULATION

With the emissivity and geometry specified as above, ray tracing calculations were carried out to compute the flux observed at infinity for an observer at a specified direction with respect to the axis of the emission region. The flux as a function of position with respect to the emission region axis is called the beaming pattern. For an axisymmetric emission region, the beaming pattern is only a function of observer polar angle with respect to the emission region axis; for a non-axisymmetric emission region, the beaming pattern depends on both polar angle and azimuthal angle of the observer.

Fig. 3 shows the beam patterns for the top and surface ring of an axisymmetric emission region on a neutron star with radius R=13.5 km, a emissivity with Gaussian width of 7.5°, a cone opening angle of 0.26 rad, and a cone height of 0.075R. Results for three different outer angles for the surface emission ring are given.

Fig. 4 shows the beam patterns for the top and surface ring of an axisymmetric emission region for the case that the surface ring has different dependencies of brightness on angle from the magnetic axis, as

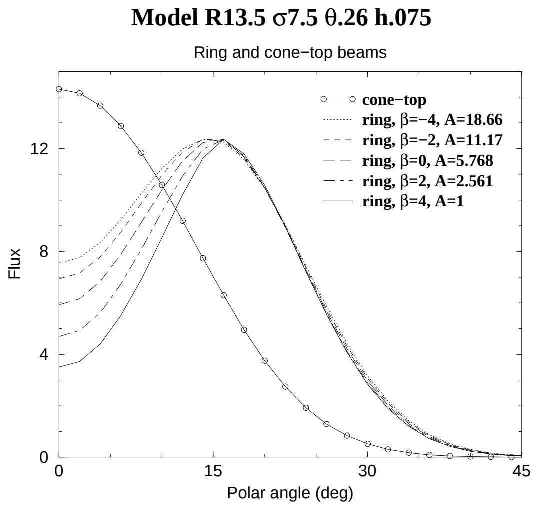

Figure 4: Beam pattern of top and ring regions, R=13.5km: dependence on power index β.

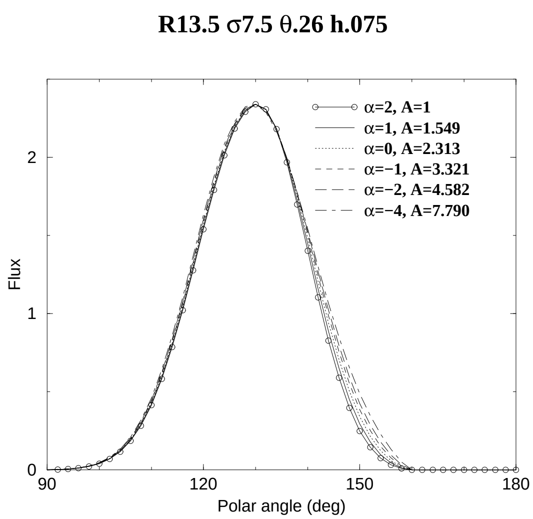

Figure 5: Beam pattern of side region, R=13.5km: dependence on power index α.

specified by the parameter β. For Fig. 4 the normalizations of the surface ring fluxes have been multiplied by the factors shown (A) so that the peaks of the beam patterns all match. This helps in comparing of the beam shapes. The surface rings which have the surface brightness peaked on the surface closer to the emission cone (larger β), suffer more from shadowing by the cone, so have a larger central dip in their beam patterns.

Next the beam pattern from the side of the emission cone is calculated. Fig. 5 shows the beam pattern from the side for different cases of the height dependence of the emissivity, as specified by α. Due to the functional form of the height dependence that was chosen, larger α values result in a larger overall flux. The fluxes were renormalized by the factors shown in

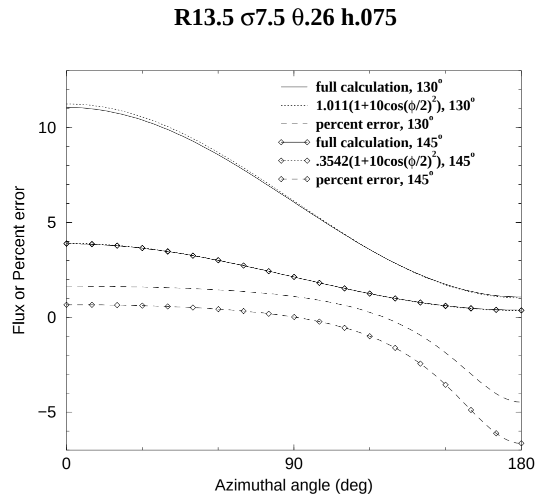

Figure 6: Azimuthal dependence of the beam pattern of the side region at two different polar angles for the case of an azimuthally-dependent emissivity (neutron star radius R=13.5km): comparison of exact and analytical approximation.

the figure caption in order to give all beam patterns the same maximum flux. The main difference in beam pattern shape is due to changes in the shadowing effect. The shadowing of the emission cone by the neutron star surface increases as the viewing angle of the observer from the cone axis increases: first the base of the cone is blocked, then progressively higher regions until the top and the entire cone is blocked. Thus cones with increasing surface brightness with height ($\alpha < 0$) are less rapidly shadowed than cones with decreasing surface brightness with height ($\alpha > 0$). However, it is seen from Fig. 5 that the effect is fairly small, even for a large change in the height dependence of the emissivity.

The above calculations were carried out for an axially symmetric emission region. Now an azimuthally-dependent emissivity is included the calculations as given by equation 4 above. Fig. 6 shows the azimuthal dependence of the beaming pattern from the side of the accretion column at polar angles of 130° and 145°. (The emission from the top and ring of the emission region are not visible at these polar angles.) The lines labelled "full calculation" include complete ray tracing to calculate the flux. The lines labelled by the analytic formulae are analytic approximations for the azimuthal dependence with normalizations fit to the curves from the full calculation. The azimuthal dependence of the beam pattern is not strongly altered from the azimuthal dependence of the emissivity. This is unlike the polar angle dependence of the beaming pattern which is strongly altered due to the light-bending.

4. DISCUSSION

Here, a more general geometry for the emission region from an x-ray pulsar has been considered than for previous model calculations. Also a spatially dependent as well as an angular-dependent emissivity is included. The goal of the calculations was to explore some of the effects of a more generalized accretion column on the beam patterns emitted by x-ray pulsars.

The beam pattern from the accretion column is the sum of the beam patterns from the various components, here, the top, the side and the surface emission ring. The top produces a pencil beam pattern beamed along the magnetic axis and the ring produces a hollow cone beam pattern with peak emission at $\sim 20°$ to the magnetic axis (e.g. Fig. 3). The cause of the dip in the ring beam pattern along the magnetic axis is shadowing by the cone. The cone side produces a fan beam peaked at polar angle larger than $90°$, due to gravitational light bending. More compact neutron stars have the peak of the fan beam at larger polar angle. For a neutron star radius of 13.5km and mass 1.4 solar masses, the peak is at $\simeq 130°$. The total beam pattern has two distinct components: a pencil beam which is the sum of cone-top and ring components and a fan beam from the side of the emission cone.

The effects of spatially dependent emissivity are as follows. The latitude dependence of the emissivity of the surface ring mainly affects the size of the central dip in the ring beam pattern. For rings which are brighter at higher latitudes, which would be expected for the case that the surface ring is heated by radiation from the cone side, the central dip is larger. The height dependence of the emissivity of the cone side affects mainly the shape of the beam pattern at polar angles larger than the polar angle of the peak of the beam pattern (Fig. 5). However, the effect is relatively weak. An azimuthally dependent emissivity produces nearly the same functional azimuthal dependence in the beam pattern. However this is not expected to hold if the emissivity is not a smooth function of azimuth.

The next stage of this work is to apply the generalized beam pattern calculation to calculation of pulse shapes and then to compare pulse shapes with those observed from X-ray pulsars.

Acknowledgments

This work supported by the Natural Sciences and Engineering Research Council of Canada.

References

[1] Leahy, D.A. & Li, L. 1995, MNRAS, 277, 117
[2] Leahy, D., 2003, ApJ, 596, 1131
[3] Kraus, U., Zahn, C., Weth, C., Ruder, H. 2003, ApJ, 590, 424
[4] Kraus, U. 2001, ApJ, 563, 289
[5] Leahy, D., 2004, MNRAS, 348, 932
[6] Leahy, D., 2004, ApJ, 613, 517
[7] Mészaros, P. & Nagel, W. 1985, ApJ, 299, 138
[8] Klein, R. Arons, J., Jernigan, G., Hsu, J. 1996, ApJ, 457, L85